SCIENCE LETTERS

ISSN: 1675-7785
eISSN: 2682-8626

Available online at
http://myjms.mohe.gov.my/index.php/sl

Science Letters 20(2) 2026, 230-256

Science Letters

Groundwater Recharge Estimation in an overexploited Alluvial Aquifer using a Combination Method; a Primary Tool for Sustainable Groundwater Management

Leila Khodapanah [1*], Negar Anvarizadeh[2], Kourosh Mohammadi[3], Surajudeen Sikiru[4*], Hassan Soleimani[1,]

[1]Department of Geoscience Universiti Teknologi, PETRONAS, Seri-Iskandar 32610 Perak Malaysia.
[2]Water resources research office, Tehran Regional Water Company, Tehran, Iran
[3]HLV2K Engineering Limited Mississauga, Ontario, Canada.
[4] School of Physics and Materials Studies, Faculty of Applied Sciences, Universiti Teknologi Mara, 40450, Shah Alam, Selangor, Malaysia

ARTICLE INFO

Article history:
Received 20 April 2026
Revised 12 June 2026
Accepted 13 June 2026
Published 30 June 2026

Keywords:
cement-based materials
microcracks
silica fume
quicklime
self-healing
sustainability

DOI:
10.24191/scl.v20i2.11382

ABSTRACT

Estimating groundwater recharge is critical for groundwater management in semiarid settings. A basic groundwater balance equation calculates the total annual groundwater recharge in the Eshtehard aquifer, north Iran, for the water year (2013–2014). The goals of this study are to (1) understand and differentiate the aquifer inflow and outflow components, (2) explicit computation of groundwater storage with the water table fluctuation (WTF) method, and (3) estimate the amount of annual Recharge in an alluvial aquifer using the water balance equation. The application of the WTF method requires a large number of water level measurements throughout the unconfined aquifer. The advantage of the method is that groundwater recharge is estimated at the scale of interest to basin hydrologic studies and that the method requires no extensive in situ instrumentation network. According to the findings of the well-log analysis, the low and high permeability zones are discontinuous and vary in depth and thickness. In the overdeveloped basin of Eshtehard, when extraction exceeds Recharge, a drawdown trend in groundwater levels may persist for many years. The yearly groundwater balance has a negative water budget of roughly 14.77 million m3/year in the aquifer system for 2013-2014. Due to the lack of permanent surface water running in the basin on the one hand and the small amount of rainfall besides the thick vadose zone in almost all parts of the plain, on the other hand, main groundwater recharge and discharge in the Eshtehard aquifer are pumping wells and recharge from returned

[1*] Corresponding author. *E-mail address*: leyla.khodapanah@gmail.com; surajudeen86@gmail.com

https://doi.org/10.24191/scl.v20i2.11382

of groundwater used for irrigation, industrial and municipal purposes. Based on this study, the overall amount of artificial groundwater removal from the alluvial aquifer is approximately 56.91 million m3/year. At the same time, the Recharge from this water is 16.48 million m3/year, percolating into the aquifer.

INTRODUCTION

Estimating and measuring groundwater recharge as an essential component of water balance is required for long-term groundwater usage in arid and semiarid settings [1]. Central and southern Iran has a semiarid climate with little annual rainfall (an average of 200 mm per year) [2]. Due to the poor quality of surface water in the study region, groundwater is an essential resource [3]. The research area is in Alborz Province, close to Iran's capital city, Tehran. The elevation varies from 1122 to 2142 meters above sea level. Based on data from the meteorological station of Eshtehard, a city in the research region (Fig. 1), during the period 1972–2019, the mean annual temperature ranges from 34°F to 97°F. It is rarely below 26°F or above 102°F [4-6]. Groundwater meets around 55% of Iran's overall water needs [7]. Groundwater overutilization has resulted in severe groundwater depletion, water level drop, the drying up of most Qanats (a gently sloping subterranean canal used to drain groundwater to the surface), and the worsening of groundwater quality in recent decades [8-10]. For example, the number of producing wells (mostly used for agricultural purposes) has grown from 47000 in 1971 to 899000 in 201,9 and about 42 percent of these wells are impermissible (IWRMC, 2019). The severe drought in Iran has further increased groundwater depletion [11]. Recharge is essential in evaluating groundwater resources and often plays a crucial role in groundwater planning [12]. Mafilika and Siyabulela Ben (2021) classified natural groundwater recharge mechanisms according to the origin into three types: direct/diffuse Recharge, localized Recharge, and indirect/non-diffuse Recharge. Each can be dominant depending on the prevailing environment. The effectiveness of these processes decreases with increasing aridity concerning rainfall distribution, soil type and plant cover [13, 14].

Many approaches have been developed for calculating the groundwater recharge, which include (a) lysimeter method, (b) soil moisture budget models, (c) water table fluctuation method, (d) catchment area water balance method, (e) numerical modeling of the unsaturated zone (f) zero flux plane method and (g) Darcy method (h) tritium profiling method and (i) chloride profiling method [15]. Notably, accurate estimation of Recharge is difficult because the processes are complex and depend on numerous local factors, including precipitation amount, intensity, duration, evapotranspiration rate, runoff, geology, soil characteristics, topography, vegetation, and land use [16, 17]. In arid and semiarid areas, the recharge estimation is more complex. The problem with estimating groundwater recharge in semiarid areas is that recharge amounts are usually small in comparison with the resolution of the investigation methods [18, 19]. The greater the aridity of the climate, the smaller and potentially more variable in space and time is the recharge flux. Direct groundwater recharge from precipitation in semiarid areas is generally small, usually less than 5% of the average annual rainfall, with a high temporal and spatial variability [20]. [18] concluded that determining groundwater recharge in arid and semiarid areas is neither straightforward nor easy. This is a consequence of the temporal variability of precipitation and other hydrometeorological variables in such climates and the spatial variability in soil characteristics, geology, topography, land cover characteristics, and land use [18]

Recharge has been estimated in arid and semiarid regions using a variety of techniques, including physical, chemical, isotopic, and modelling processes, for example, Chloride Mass Balance (CMB), Water Balance model (WBM), tritium tracer (3H) and Water-Table Fluctuations (WTF). These techniques have been described in previous studies and reviews, focusing primarily on semiarid regions [15]. According to these studies, the purpose of recharge studies has dictated, to some extent, the method used to estimate Recharge and the scale of the studies. Regional recharge estimation for water resources evaluation has relied mostly on groundwater-based approaches, which integrate over large spatial scales and generally

https://doi.org/10.24191/scl.v20i2.11382

cannot be used to estimate local variability in Recharge. [18] Different studies focus primarily on techniques for estimating Recharge and provide applications and case studies in semiarid regions. These studies showed that rainfall below 200 mm usually results in negligible Recharge [21]. Different researchers have conducted groundwater recharge studies in arid and semiarid regions of Iran [22-25]. According to this research, two recharge estimation methods commonly used for arid and semiarid regions include the water budget method (WBM) and the water table fluctuation (WTF) method [26]. In this study, a combined approach of WBM and WTF has been applied for groundwater recharge estimation in the Eshtehard region [27]. The estimation of the groundwater balance of a region is generally equal to quantifying all individual inflows to or outflows from a groundwater system and changes in groundwater storage over a given period. The groundwater balance method has been successfully used in the semiarid alluvial aquifers around the world and Iran [28-30]. The water table fluctuation technique (WTF) links the change in groundwater storage with resulting water table fluctuations through the storage parameter (specific yield in an unconfined aquifer). This method is considered one of the most promising and attractive due to its accuracy, ease of use, and low application cost in semiarid areas [21] . The WTF method was first used to estimate groundwater recharge and has since been used in numerous studies for the same purpose or for groundwater storage changes estimation [31, 32].

This study lies in the integrated application of the Water Budget Method (WBM) and Water Table Fluctuation (WTF) method to estimate groundwater recharge and evaluate the annual groundwater balance of the Eshtehard Plain, a groundwater-dependent and data-scarce semiarid region of central Iran. Unlike previous studies that primarily focused on recharge estimation using a single approach, this research combines complementary methods to improve estimation reliability while simultaneously quantifying groundwater storage changes, pumping withdrawals, lateral groundwater flows, and safe annual yield. The study provides a practical and transferable framework for groundwater assessment and sustainable management in arid and semiarid regions experiencing severe groundwater depletion and limited hydrogeological data availability.

STUDY AREA

Location and climate

This research focuses on the hydrogeologic profile of the Eshtehard basin, which is located in the Alborz Province and adjacent to the capital city of Iran (Figure 1). The study area is about 100 km southwest of Tehran and lies between 50^0 10' to 50^0 47' longitudes and 35^0 34' to 35^0 47' latitudes. The Eshtehard basin is characterized by a long, west-east trending plain, extending from just east of Bouein Zahra and Haji Arab basin into Karaj Plain. Upland plateaus and mountains surround this long, narrow plain. Surface elevations in Eshtehard Basin range from approximately 1122 to 2142 meters above sea level (m.a.s.l.). This area has a population of approximately 30000 by the 2016 Iran Census and a total land area of about 480 km^2. It is considered one of the promising areas for the industrial and agricultural centre in the Alborz province. The Halghehdar Mountains bound the study area in the north and the Kordha and Ghezelban Mountains in the south. Karaj plain defines the eastern boundary, and Haji Arab Plain defines the western boundary of the study area. The study area's most important towns and villages are Eshtehard, Sehat Abad, Jafar Abad, and Mehdi Abad. The study area can be accessed through the Tehran-Karaj Road toward the Eshtehard or the Shahriar road [3].

https://doi.org/10.24191/scl.v20i2.11382

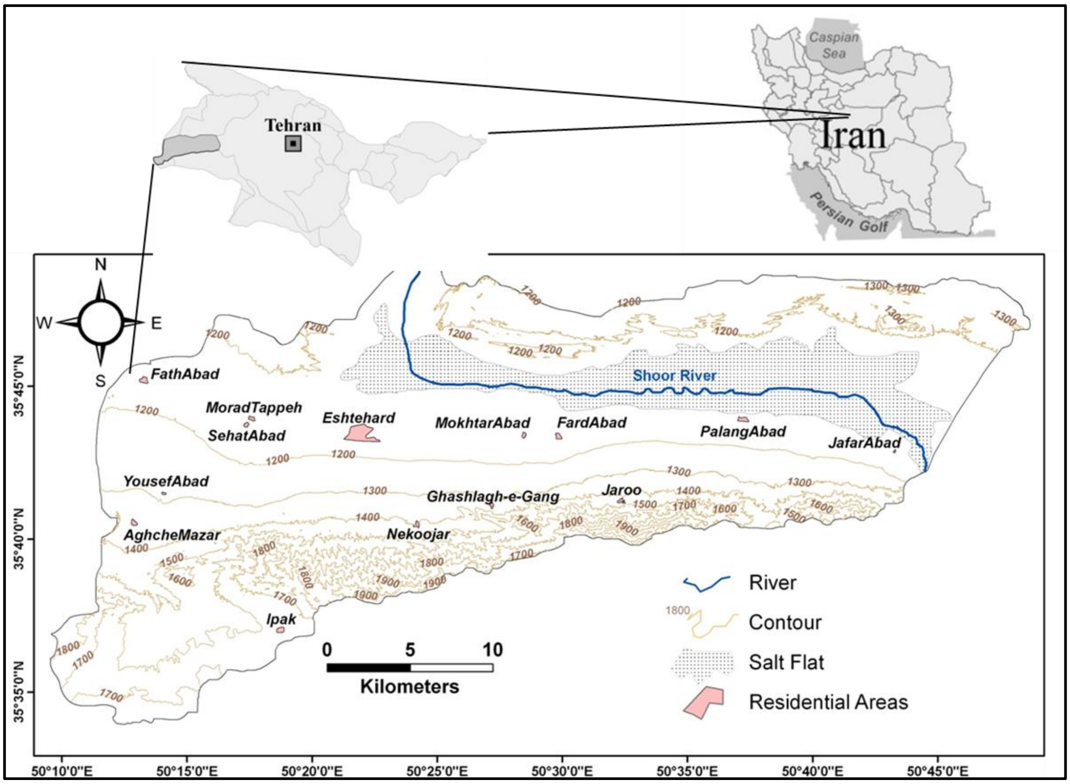

Fig. 1. The geographical location of Eshtehard Plain in west Tehran

Iran lies within the arid and semiarid climatic belt. Most central and southern Iran is within the semiarid part of Iran, which is dominated by low precipitation and high potential evapotranspiration with no permanent streams [33]. Eshtehard in central Iran has such a climatic condition. The climatological investigations of the study area are based on the available data measured by climatological and synoptic stations of Alborz and Tehran Province. Data for rainfall, temperature, and humidity were obtained from the records at nineteen meteorological and synoptic stations within the Eshtehard basin and adjacent basins provided by the Iran Water Resources Management Company and Iran Meteorological Organisation (IWRMC, 2019). According to Demarton and Emberger's climate classification [34], the climate in the Eshtehard Basin is continental, with chilly winters and scorching summers [35]. Summer rain falls from June to October, with wetter spells occurring in the winter and spring. The average annual precipitation for the study region is 227.4 (214.8) millimetres, according to long-term monthly and annual rainfall data collected between 1997 and 2019. In 2018, the yearly rainfall was 329.1.5 mm, while in 2010, it was 133.9 mm (Figure 2a). From February to May, the wet season is in effect. Winter is the rainiest season of the year, with 22.2 percent of the total rainfall occurring in March and 16.2 percent in April. Figure 2b shows that the highest and lowest monthly rainfall amounts were 50.4 and 0.3 mm, respectively, in March and September.

https://doi.org/10.24191/sl.v20i2.11382

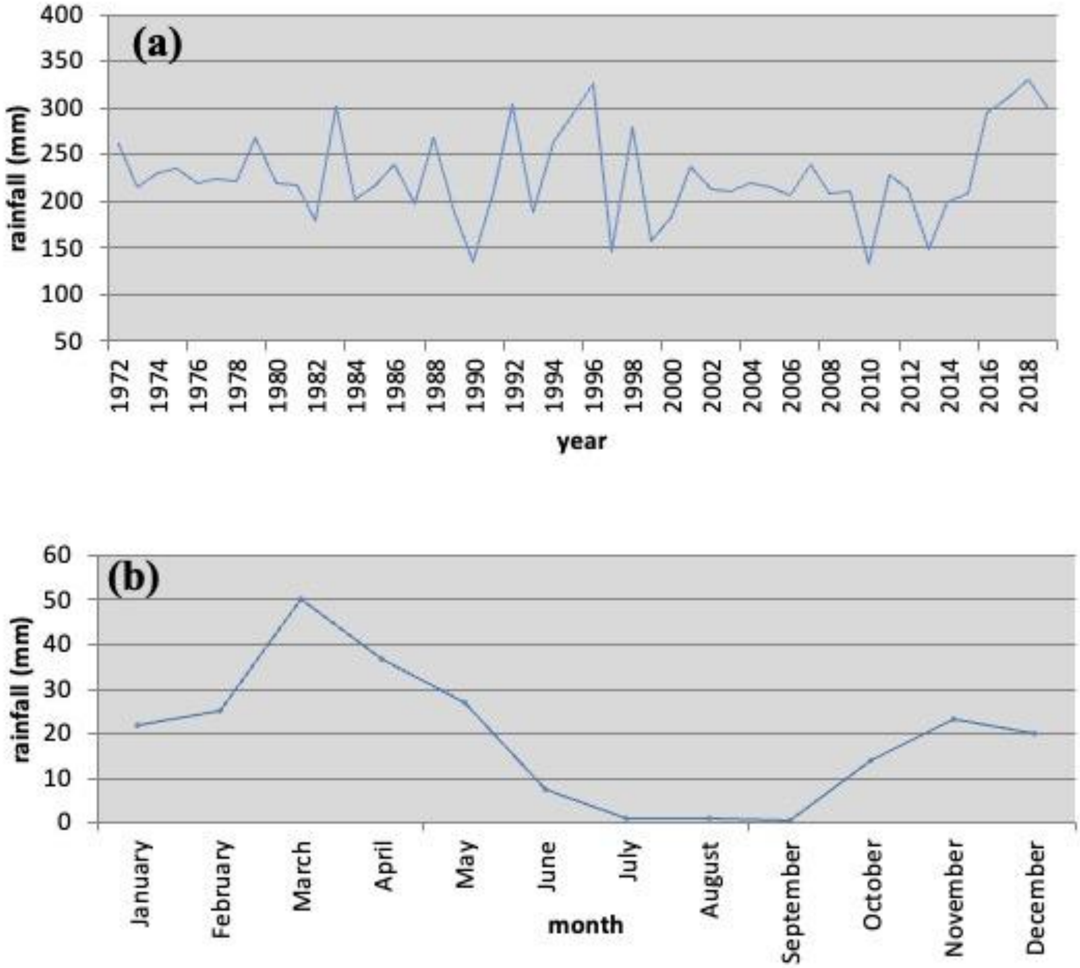

Fig. 2. (a) The annual variations of rainfall in the study area from 1972 to 2019 (After IWRMC, 2019) (b) The average monthly variations of rainfall in Eshtehard. (After IWRMC, 2019)

It is not uncommon for the region to experience drought, with yearly deficits of up to 1170 millimetres of water. Runoff consequently tends to be very low. The temperature in the Eshtehard area is highly varied between summer and winter, with mean monthly values highest during July and August and lowest in December. Throughout January, the average low is -9.7°C, and during July, it's an uncomfortable 40.4°C on average. Long-term data indicates that the research area's yearly average temperature is 14.7°C (IWRMC, 2019). Fig. 3. illustrates the absolute maximum, minimum, and average monthly temperature between 1972 and 2019.

https://doi.org/10.24191/scl.v20i2.11382

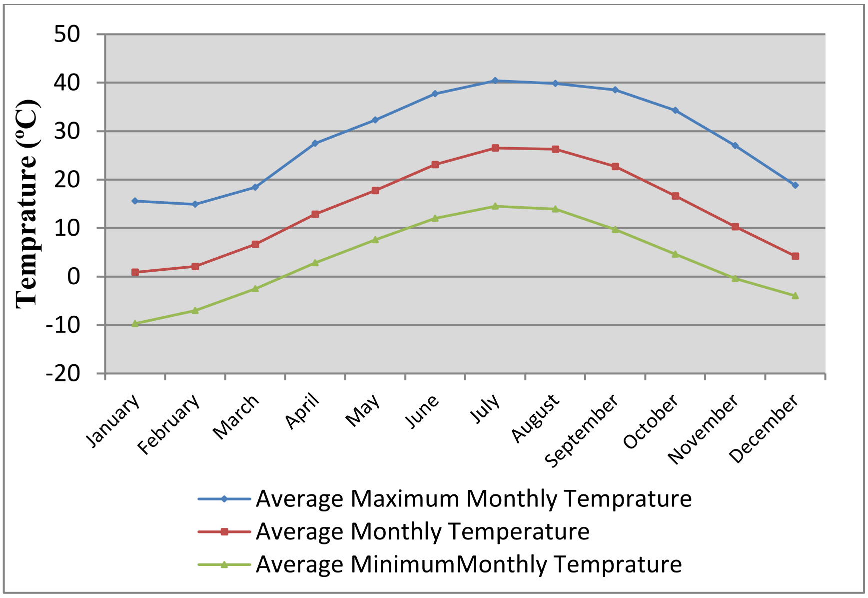

Fig. **Error! No text of specified style in document.**. The Average, maximum, and minimum monthly temperature of the study area for the period of 1972 to 2019 (After IWRMC, 2019)

Iran Water Resources Management Company developed evapotranspiration estimates from 2005 to 2019 based on evaporation measurements at a referral station near the Eshtehard basin (KarimAbad station) and using the iso-evaporation maps. According to climatological data, the monthly relative humidity in the research area ranges from 35% in June to 72% in January. In addition, it shows that the plain's annual potential evaporation is around 1395.7 mm (Table 1). The precipitation gradient is reversed, with less evapotranspiration north and south and more in the basin's centre. This peak in potential evaporation occurs during July when the wind speed is at its highest, daylight hours are the longest, and humidity is at its lowest. Lows of 32.9 mm are common in January when the days are shorter, the nights are longer, and the relative humidity is higher (IWRMC, 2019).

Table 1. Mean monthly and annual evaporation of the Eshtehard Basin (After IWRMC, 2019)

Basin Mean Elevation (m amsl)	Evaporation	Oct	Nov	Dec	Jan	Feb	Mar	Apr	May	Jun	Jul	Aug	Sep	Annual
1313	Pan evaporation	235.5	122.7	74.0	55.8	55.2	72.6	140.4	248.5	361.0	452.5	460.1	381.6	2659.9
	Evaporation from the water's surface	164.8	85.9	51.8	39.1	38.7	50.8	98.3	174.0	234.6	271.5	276.0	229.0	1714.5
	Potential Evaporation	98.5	58.5	35.2	32.9	45.8	71.1	117.9	158.7	204.9	220.3	196.7	155.2	1395.7
Mean monthly pan evaporation (percent)		8.9	4.6	2.8	2.1	2.1	2.7	5.3	9.3	13.6	17.0	17.3	14.3	100.0
Mean monthly potential evaporation (percent)		7.1	4.2	2.5	2.4	3.3	5.1	8.4	11.4	14.7	15.8	14.1	11.1	100.0
Class A evaporation pan coefficient		0.70	0.70	0.70	0.70	0.70	0.70	0.70	0.70	0.65	0.60	0.60	0.60	0.67

https://doi.org/10.24191/scl.v20i2.11382

Geological setting

The North Tehran Thrust, which runs from east-west up to northwest-southeast, is part of the depression and is regarded as the continuation of the Tehran plain. It is between (central) Alborz and central Iran tectonic zones (Darvishzadeh, 2003). Generally, it can be said that it is in a structural-sedimentary unit of central Iran and has the same main characteristics, including tectonic, stratigraphic, magmatism, and metamorphism characteristics of central Iran. The area has been mapped by the Geological Survey of Iran (GSI) (2000) at a 1:100000 scale. The geology has been described by Aghanabati (2004) and Yousefi et al. (2000). Eocene through Miocene, Plio-Quaternary, and Quaternary deposits cover the study area's stratigraphic succession from bottom to top (Figure 4). According to a geological map produced by the Geological Survey of Iran, these formations are categorized as follows (Table 2).

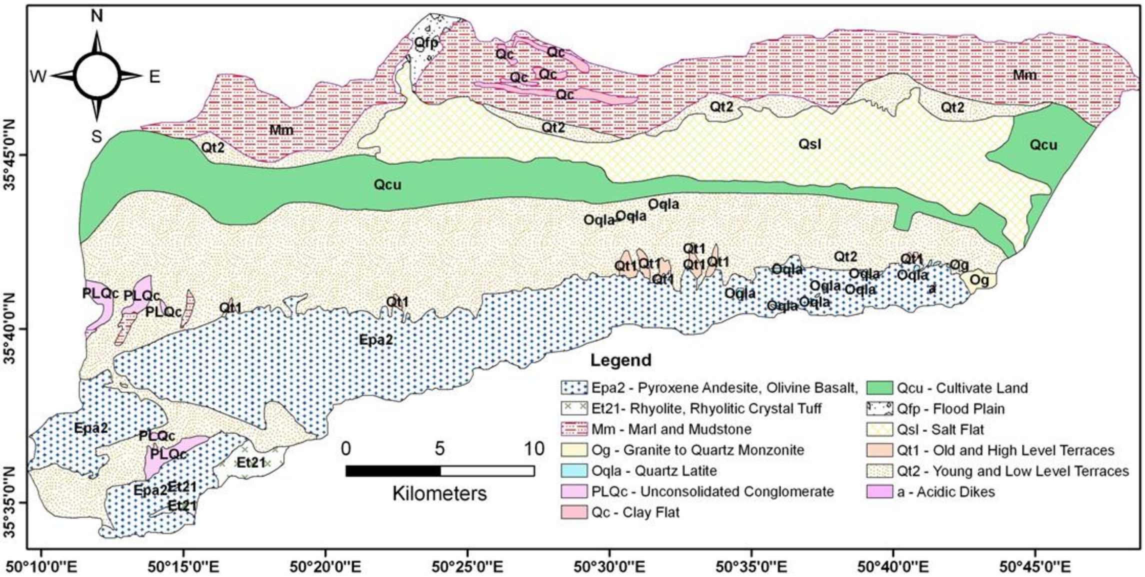

Fig. 4. The geological map of the study area (modified after GSI, 2000)

https://doi.org/10.24191/scl.v20i2.11382

Table 2. Stratigraphic column of the study area (modified after GSI, 2000)

Quaternary			Qt2	Young and low-level terraces	Qcu	Cultivated land	Qfp	Flood plain	Qsl	Salt flat	Qc	Clay flat
Quaternary			Qt1	old and high-level terraces								
Quaternary / Neogene	Mio-Pliocene		PLQc	Unconsolidated conglomerate with intercalations of sand, silt, and clay								
Neogene	Mio-Pliocene		Mm	Gypsiferous marl and mudstone with intercalations of sandstone and gypsum								
Paleogene	Eocene	Upper	Oqla	Quartz latite								
Paleogene	Eocene	Upper	Og	Granite to quartz monzonite								
Paleogene	Eocene	Upper	Epa2	Porphyritic pyroxene andesite, olivine basalt, andesitic basalt, grey volcanogenic sandstone, porphyritic trachytic to andesitic								
Paleogene	Eocene	Middle	Et21	Rhyolite, rhyolitic crystal tuff								
Paleogene	Eocene	Middle	a	Acidic dikes								

Eshtehard Plain is located between the north (Halgheh Dar) and south (Kouh Kordha, Jarou, Ghosh Gouni, etc.). North heights solely include Neogene deposits, and south heights, which lie in the "Oroumieh-Pole Dokhtar" volcanic belt, are generally of Middle and Late Eocene volcanic rocks (lava and pyroclastic). Due to the closeness and common border with central Alborz, it is under the influence of this zone's newly formed and young thrusts. The superiority of faulting over folding is among the characteristics of this zone. Middle Eocene formations mainly consist of green pyroclastic, often tending to blue. In higher horizons, these green tuffs are changed into cream rhyolite tuffs. With their dark colours, the upper Eocene stones can be easily distinguished from the green series of Middle Eocene deposits [36, 37]. This series, which lies on the green series of Middle Eocene in a concordant manner, consists of Andesite and lateritic lavas. Rhyolite domes and lavas have less development. Despite the Middle Eocene green series indicating submarine volcanism, the upper Eocene series shows continental to shallow (coastal) marine volcanism. Late Eocene stones series in the zone have been divided into lower, intermediate, and upper sections, which are very similar in terms of permeability, the possibility of aquifer formation, erosion, etc. Granite masses whose age ranges from Late Eocene – Oligocene to lower Oligocene have relatively large gradation, indicating slow cooling [38]. Oqla unit, related to Late Eocene and its outcrop, may be observed dispersedly in different areas of the east part of south heights and is of quartz latite type [39]. In the north heights of Eshtehard (Halgheh Dar), Neocene begins with red detrital-evaporite deposits, which lie on Eocene volcanic units unconformably. Neogene deposits of this study area have been divided into different units, which lack any importance in relation to permeability, feeding, or formation of the aquifer.

https://doi.org/10.24191/scl.v20i2.11382

Plio-Quaternary (Plqc) unit lies with a high unconformability on Neogene sedimentary deposits and mainly includes consolidated conglomerate (GSI, 2000). The kind of grains of this conglomerate mainly consists of Eocene volcanic and Oligocene granite, in which some interbeds of sand, silt, and clay may be seen. The bedrock of southwest areas mainly consists of this unit. A set of Quaternary deposits developed throughout the plain and in the neighbourhood and amplitudes of mountains. Alluvial deposits have coarse grains in amplitudes, and the number of refined grains, i.e., fine sand, silt, and clay, increases gradually towards the middle and down of the plain and, finally, the edge of Eshtehard salt flat. Old Quaternary deposits (Qt1) include alluvial deposits of sand and cobbles with different cohesion and sand cement, bad sorting, and non-homogeneous grains that may be considered an unconsolidated conglomerate. The material of the grain is mainly Eocene volcanic rocks. Younger alluvial deposits (Qt2) include a set of Eocene volcanic pebble, sand, silt, and clay whose terrane includes Neogene and Eocene igneous rocks (Yousefi et al., 2000). This alluvial unit is also considered a terrace or young alluvial fans. It is important because a significant part of Eshtehard aquifer saturated layers have been formed in it. One of the characteristics of south Heights is the superiority of faulting over folding. In the south of north heights (Halgheh Dar), the Eshtehard thrust causes the Neogene deposits to cover over recent alluviums. A limited number of anticlines and synclines have been formed in the north and south.

MATERIALS AND METHODS

Well log analysis

Analysis of observation well logs and core samples can provide information on the subsurface geology, vertical sequence and hydrogeologic grouping of deposits, geological age, paleoenvironment for depositional history, and geological correlations. Tehran Regional Water Company (TRWC, 2019) has drilled 24 observation wells up to 143 m into the Eshtehard aquifer (Table 3). These wells provide a unique opportunity to study the aquifer media and sequence of alluvial strata and depth to the water table and base of the aquifer. Also, this information can be derived from existing production well logs collected in the TRWC well database. The boreholes stratigraphic column of logged wells in selective parts of the plain.

Analysis of 20 selected well logs in the study area has been summarized in Tables 4. and 5. Table 6 shows each layer's detailed description (lithology and thickness) in every stratigraphic column. In Table 5, each sampling column has been divided into two parts, saturated and unsaturated zones, and the percentages of different particle sizes have been calculated for each zone separately. The well-sampling records indicate that the surficial zone in most plain parts has been covered mainly through the uppermost layers of clay, silt, and sand. The thickness of the top layer ranges approximately from 1 to 50 m. The body of the aquifer is formed by a mixture of gravel, boulder, sand, silt, and clay. Considering borehole analysis, it can be deduced that the aquifer is a heterogeneous-unconfined system with a different thickness of alluvium deposits.

In this study, the layers in each stratigraphic column have been categorized into six groups: clayey, silty, sandy, gravely, pebbly and conglomerate. After classification, the geological texture of each well was evaluated by quantifying the percent of the total thickness of each group in the sampling thickness of the well. The results show that the total thickness of clayey and gravely layers in the logged wells are relatively more than the other layers (Table 6). The maximum thickness of clayey layers in the stratigraphic column was observed in the observation wells of Jadde Jaroo (OW15) and Jadde Mohammadyar (OW10), reaching about 107 and 102 meters, respectively. In observation wells OW5, OW 14, and OW16, the thickness of clayey layers reaches 100% of the sampling thickness, while the depth of the well in all of them is less than 66 meters. Silty and conglomerate layers have the minimum total thickness in the logged wells. The maximum thickness of these layers was seen in the observation wells of Jonoube Roostay e Fard Abad (OW13) and Jadde Jaroo (OW15), respectively.

https://doi.org/10.24191/scl.v20i2.11382

Table Error! No text of specified style in document.**.** Specification of the observation wells in the study area

No	Well Name*	Location	Coordinate (UTM) X	Y	Well** Elevation (a.m.s.l.)	Well** Depth	Mean** Water Depth
1	OW1	Jonoub e Fath Abad	35° 43.'	50° 12.'	1208.32	NA	60.67
2	OW2	Yousef Abad	35° 42'	50° 13'	1265.26	NA	124.2
3	OW3	Gheshlagh e Morad Tappeh	35° 44'	50° 16'	1175.98	NA	26.17
4	OW4	Gharb e Shahrak e San'ati	35° 42'	50° 16'	1199.18	134	80.65
5	OW5	Shargh e Sehat Abad	35° 43'	50° 17'	1168.83	66	6.41
6	OW6	Shargh e Shahrak e San'ati	35° 42'	50° 20'	1237.95	140	106.03
7	OW7	Gharb e Eshtehard	35° 43'	50° 20'	1183.95	NA	48.33
8	OW8	Jonoub e Eshtehard	35° 42'	50° 22'	1223.62	136	83.86
9	OW9	Shargh e Eshtehard	35° 43'	50° 23'	1163.46	59	18.64
10	OW10	Jadde Mohammadyar	35° 41'	50° 25'	1265.87	142	115.86
11	OW11	Shargh e Emamzade Soleiman	35° 43'	50° 26'	1150.66	42	12.15
12	OW12	Jadde Ghale Afshar	35° 42'	50° 28'	1222.6	102	70.42
13	OW13	Jonoube Roostay e Fard Abad	35° 41'	50° 28'	1209.26	78	58.14
14	OW14	Shargh e Fard Abad	35° 43'	50° 30'	1149.26	30	0.7
15	OW15	Jadde Jaroo	35° 42'	50° 32'	1289.72	143	119.37
16	OW16	Mehdi Abad	35° 44'	50° 32'	1146.66	28	2.9
17	OW17	Jadde Yeklang	35° 43'	50° 35'	1210.6	84	58.59
18	OW18	Palang Abad	35° 44'	50° 36'	1147.32	50	3.25
19	OW19	Jadde Gamargan	35° 43'	50° 38'	1202.19	85	55.57
20	OW20	Hashiye e Roodkhan e Shoor	35° 44'	50° 38'	1135.59	45	2.36
21	OW21	Gol Dasht	35° 43'	50° 39'	1180.62	62	41.03
22	OW22	Fadak	35° 43'	50° 40'	1147.03	38	5.87
23	OW23	Jonoub e Jafar Abad	35° 42'	50° 42'	1177.17	64	38.75
24	OW24	Jafar Abad	35° 44'	50° 44'	1134.68	38	2.83

*Note: Well Name assigned arbitrarily
**in meter
NA: Not Available

https://doi.org/10.24191/scl.v20i2.11382

Because of their high porosity and permeability, sand and gravel deposits have higher hydraulic conductivity than clay and silt. Therefore, higher hydraulic conductivity is expected in the Eshtehard aquifer, where coarse grains of alluvium deposits dominate the refined grains. Such areas are consistent with the main production zones where most production wells are located.

Table 4. Summary of the analysis of logged wells in the study area

Well Name	Percentage of layer thickness in the unsaturated zone						Percentage of layer thickness in the saturated zone					
	Clayey Layer	Silty Layer	Sandy Layer	Gravely Layer	Pebbly Layer	Conglomerate Layer	Clayey Layer	Silty Layer	Sandy Layer	Gravely Layer	Pebbly Layer	Conglomerate Layer
OW4			44	56						100		
OW5	100						100					
OW6		9	35	23	33						100	
OW8			79	21					6		94	
OW9	32			68			75		12.5	12.5		
OW10	83.5			14		2.5	19			54		27
OW11	25			75			100					
OW12	56			39		5	6				84.5	9.5
OW13		86		14						100		
OW14	100						100					
OW15	84			8.5		7.5	29			29		42
OW16	100						100					
OW17	51			41		8	44			56		
OW18			100				85			15		
OW19	82			18			83			3		14
OW20		100					53.5	46.5				
OW21		12		59	29			43			57	
OW22	100						50			50		
OW23	69			31			32			40		28
OW24		100					51	49				

Note: Wellname assigned arbitrarily

https://doi.org/10.24191/scl.v20i2.11382

Table 5. Summary of the aquifer media assessment of the logged wells in the study area

Aquifer Media (Based on the total thickness of each layer in meters)		OW4	OW5	OW6	OW8	OW9	OW10	OW11	OW12	OW13	OW14
Clayey layers	C+S					31	39				
	C+G+S					5					
	C+Si+S		66				3	2	3		10
	C+S+G						17	9	19		11
	C+S+Si							9			
	C							10			
	C+M						5	3			4
	C+S+G+P										5
	C+S+Si+G										
	C+G+S+P						38		19		
	C+G+P+S										
	C+Si+S+G										
Silty Layers	Si+C+G+S			10							
	Si+C+S									50	
Sandy Layers	S+G+C+Si	36									
	S+G+Si+C			24							
	S+G+P+Si+C			13							
	S				69						
	S+C+G					5					
	S+Si+G+C										
Gravely layers	G+S+Si+C	98									
	G+S+P+Si+C			24							
	G+S+C+Si				18						
	G+S+C+P					9	12	9			
	G+S+P+C					9					
	G+S+C						7		27		
	G+P+C+S						10				
	G+P+S+C										
	G+P+S+Si+C									28	
Pebbly layers	P+G+S+Si+C			69	49						
	P+G+S+C								17		
	P+Co+G+S+C								10		
	P+G+S										
	P+G+S+C+Si										
Conglomerate Layers	Co						3		7		
	Co+P+G+B						7				
	Co+P+G+S+B										
	Co+P+B										

Note: C=Clay; Si=Silt; S=Sand; G=Gravel; P=Pebble; Co= Conglomerate; B=Boulder

https://doi.org/10.24191/scl.v20i2.11382

Table 6 (Continued). Summary of the aquifer media assessment of the logged wells in the study area

Aquifer Media (Based on the total thickness of each layer in meters)		OW15	OW16	OW17	OW18	OW19	OW20	OW21	OW22	OW23	OW24
Clayey layers	C+S	70	11	17						9	
	C+G+S					24					
	C+Si+S				10	6					
	C+S+G	26			24	40			12	23	
	C+S+Si										
	C		4	13							
	C+M		4		6		23		7		18
	C+S+G+P										
	C+S+Si+G		9						3		
	C+G+S+P										
	C+G+P+S	12		12							
	C+Si+S+G									3	
Silty Layers	Si+C+G+S						22				
	Si+C+S							14			20
Sandy Layers	S+G+C+Si										
	S+G+Si+C										
	S+G+P+Si+C										
	S										
	S+C+G										
	S+Si+G+C				3						
Gravely layers	G+S+Si+C							24			
	G+S+P+Si+C										
	G+S+C+Si										
	G+S+C+P				7				6		
	G+S+P+C								7		
	G+S+C	10		14						4	
	G+P+C+S			24							
	G+P+S+C	7				11				18	
	G+P+S+Si+C										
Pebbly layers	P+G+S+Si+C										
	P+G+S+C										
	P+Co+G+S+C										
	P+G+S							12			
	P+G+S+C+Si							12			
Conglomerate Layers	Co	10		5		4				3	
	Co+P+G+B										
	Co+P+G+S+B	8									
	Co+P+B									4	

Note: C=Clay; Si=Silt; S=Sand; G=Gravel; P=Pebble; Co= Conglomerate; B=Boulder

The results of the well-log analysis indicate that low and high permeability zones are discontinuous and variable in depth and thickness. In most vertical profiles of the aquifer, sandy and gravely layers have been interbedded with various mixtures of lower permeability silt and clay deposits. In some parts, the low permeability layers of clay and silt are lithologically inconsistent and include various mixtures of higher permeability sand and gravel sediments. Thus, in these areas, the low-permeability layers are very leaky, porous, and hydraulically interconnected throughout.

https://doi.org/10.24191/scl.v20i2.11382

Hydrogeology

Eshtehard Aquifer, one of the essential groundwater systems of Alborz province, is an elongated aquifer that extends west-east. The aquifer has mainly consisted of alluvial successions deposited on the eroded surface of the Miocene basements. To the north, the aquifer is locally bounded by basement outcrops. The south boundary is limited to the middle and late Eocene formation; the west and east side boundaries are along Haji Arab Plain and the Karaj Plain, respectively. Based on available geoelectrical cross sections (Khodapanah et al., 2019), geological survey, and well logs data, it is defined that the study area contains an unconfined Quaternary alluvial aquifer composed of a sequence of relatively coarse-grained gravel and sand interconnected with silt and clay. Based on the geo-electrical investigation, log of deep wells, and bedrock core examination, the bedrock predominantly consisted of Marl, shale, and sandstone of the Miocene era. Based on the isopach map of alluvial deposits thickness, the aquifer has a maximum thickness of 175 m in the middle parts of the plain and a minimum thickness of 25 m in the periphery of the study area. The average aquifer thickness varies from 50 to 125 m (Khodapanah et al., 2019). Groundwater in the study area generally flows northward and northeastward from the recharging area toward the Shoor River. The most productive part of the aquifer, coincident with more groundwater exploitation regions, is south of Eshtehard city toward the western boundary of the aquifer. Unfortunately, the highest annual drop in groundwater levels occurred in this part, and the aquifer is in critical condition.

Hydraulic characteristics of aquifer

One of the essential aspects of groundwater resources investigation is the determination of aquifer properties. Several methods are available in groundwater hydrology for the evaluation and estimation of the hydraulic characteristics of aquifers, like transmissivity, hydraulic conductivity, and storability (Singhal & Gupta, 2010). The most used methods involve pumping tests on existing or newly drilled wells followed by analysis and interpretation of pumping test data [40]. Before a pumping test is conducted, all available geological and hydrological information like the type of aquifer, thickness and lateral extent of the aquifer, and data on regional groundwater flow should be collected. However, it should be appreciated that such tests are both capital and labour-intensive, requiring several boreholes, many operatives, and a considerable amount of equipment (Osborne, 1993). Furthermore, the estimation of hydraulic conductivity is crucial for the reliable simulation of the groundwater flow of one aquifer [41]. The various formulas available for calculating aquifer characteristics from pumping test data are valid only if various assumptions about aquifer continuity, thickness, homogeneity, isotropy, well storage, and the nature of the fluid flow are valid under field conditions.

The application of the geoelectrical method has led researchers to develop surface resistivity techniques for making quantitative estimates of aquifer properties such as yield, hydraulic conductivity, and transmissivity [41]. The relation between transverse resistance (R) and transmissivity (T) is one of the activities used to derive hydraulic properties using geoelectric data, which has been applied in the study area [39]. Based on the Transverse Resistance map from the geoelectrical investigation, the transmissivity variation map in the Eshtehard aquifer was provided (Figure 5) [39].

According to this map, two regions with high transmissivity can be recognized. One of these regions is west of the study area (south of FathAbad and north of YousefAbad and AbBarik), with a transmissivity of about 2000 m^2 /day. Another region with the same transmissivity is in the west and southwest of Eshtehard City. The discharge rate of production wells in these two regions mostly ranges between 30 to 60 litres per second. Transmissivity coefficient values decrease from west to east. The reason for decreasing the transmissivity coefficient values from central parts (in the west-east direction) toward the north is different from the south. It reduces toward the south due to high bedrock elevation, thinner alluvial deposits, and a saturated zone. While toward the north, in addition to increasing the bedrock elevation, the prevailing fine grain size in alluvium has resulted in less transmissivity coefficient values in the northern parts.

https://doi.org/10.24191/scl.v20i2.11382

Generally, the transmissivity in the plain varies from 500 (m^2/day) in the north part of the area to 4000 (m^2/day) in the middle part of the plain (Abkhan, 2013). Due to lack of drilling exploratory wells and pumping test data in the study area, the accurate rates of storage coefficient of the aquifer in different parts are not available. According to Abkhan (2013), this coefficient is estimated to be about 18% based on other hydrogeological conditions such as southern highs lithology, expansion of alluvial fans, texture of aquifer, results of groundwater balance calculation, groundwater level fluctuation, and above all storage coefficients of two pumping test conducted near the southwest boundary in the adjacent basin (with storage coefficients of 16% and 20%) (Abkhan, 2013).

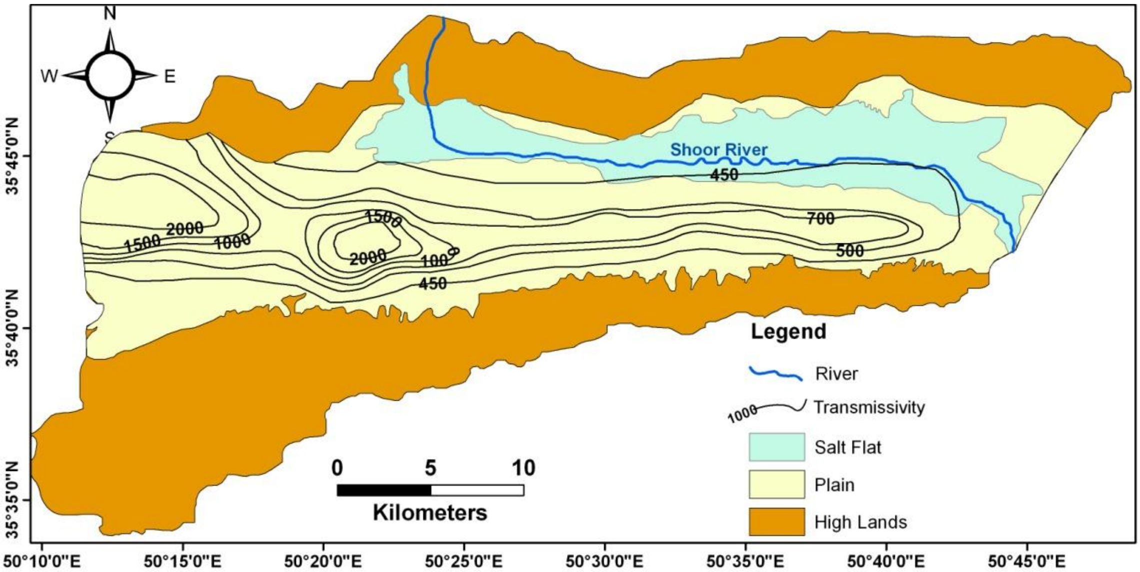

Fig. 5. The Transmissivity map of Eshtehard Aquifer

Groundwater Level Fluctuations

Groundwater level fluctuations can result from various hydrological phenomena, some natural such as groundwater recharge, evaporation, and metrological phenomena, and some human-induced such as groundwater pumping, deep well injection, artificial Recharge, agricultural irrigation, and drainage. There may be more than one mechanism operating simultaneously; therefore, the various phenomena must be understood. The time variations in groundwater levels can be considered as (1) long-term, (2) seasonal, and (3) short-term in duration. In overdeveloped basins, where extraction exceeds Recharge, a drawdown trend in groundwater levels may continue for many years. Seasonal fluctuations usually result from influences of rainfall, bank storage, and pumping for irrigation, all of which follow well-defined seasonal cycles [42]. Water level data monitored by Teheran Regional Water Company (TRWC, 2019) was used for water level trend analysis of the study area. Two groundwater maps were provided using monitored data: depth-to-groundwater and groundwater elevation—the data used for long-term trend analysis and map preparation showing changes in the groundwater regime. Monthly fluctuations in groundwater level have been measured in the Eshtehard alluvial aquifer since 1997. The locations of the 24 groundwater level monitoring wells in this aquifer are shown in Figure 6. In this study, to analyze the monthly spatial and temporal variations in groundwater levels, groundwater level records of the observation wells from October 1997 to October 2019 were used.

https://doi.org/10.24191/scl.v20i2.11382

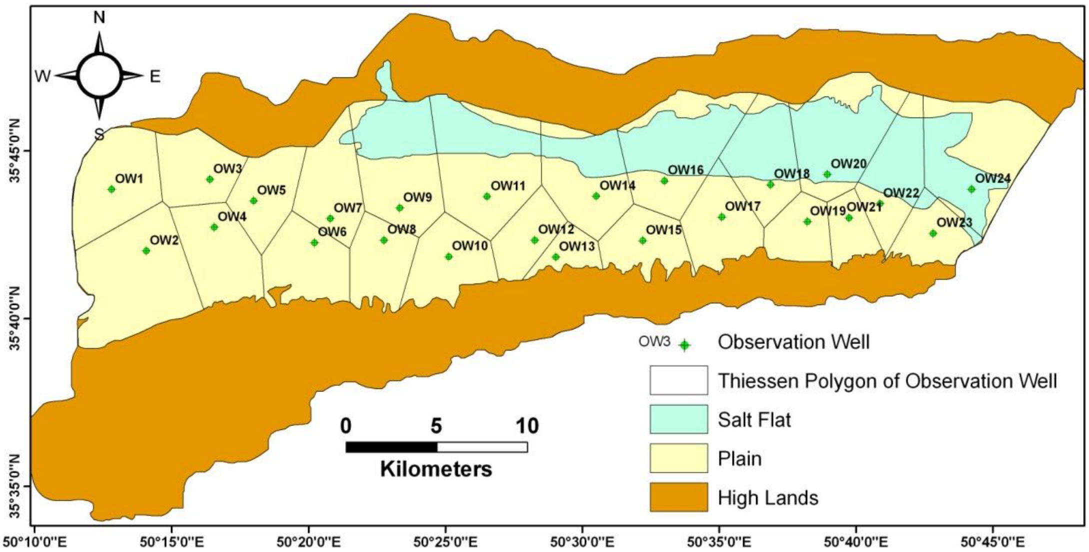

Fig. 6. The Geographical locations of the observation wells

Long-term and seasonal average areal water-level fluctuations recorded in the monitoring wells are plotted in Figure 7. The mean values are calculated by creating Thiessen polygons for the monitoring wells (Figure 6). The seasonal fluctuations and long-term decline of groundwater levels in the area are evident in this average areal well hydrograph. The monthly hydrograph for observation wells during the study period has been analyzed. Based on the chart, a generally continuous decrease in mean groundwater level during the study period is considerable. As reflected in the chart, the mean groundwater level at different times fluctuates from 1151.4 to 1136.2 m, and the minimum and maximum have been usually recorded in October and April, respectively (Figure 7). It also shows that the mean groundwater level in the plain declined by about 15.2 m from October 1997 to October 2019 with an average of about 0.69 meters. During the wet and dry periods, the groundwater levels of the study area show an approximate seasonal pattern of fluctuation. This results from influences such as rainfall and evapotranspiration that follow well-defined seasonal cycles. Based on climatological information, high groundwater elevation in early winter is expected to coincide with periods of minimum evapotranspiration, minimum well extraction, and maximum precipitation. Low groundwater elevation conversely, occurs in late summer.

According to data on groundwater depth, the depth to the water level in Eshtehard ranged between 0.6 m and 130 m below ground level. To investigate the spatial distribution of groundwater level, a map of groundwater depth and elevation has been prepared for the period between October 2001 and January 2019 using Arc GIS 9.2. These maps were based on the average groundwater levels or groundwater depths of 24 observation wells. The groundwater level (or depth) was interpolated in the ArcMap (geostatistical analyst extension) using Kriging [43]. The groundwater depth map and elevation are presented in Figure 8 and figure 9, respectively. These data and the produced map reveal the following details.

https://doi.org/10.24191/scl.v20i2.11382

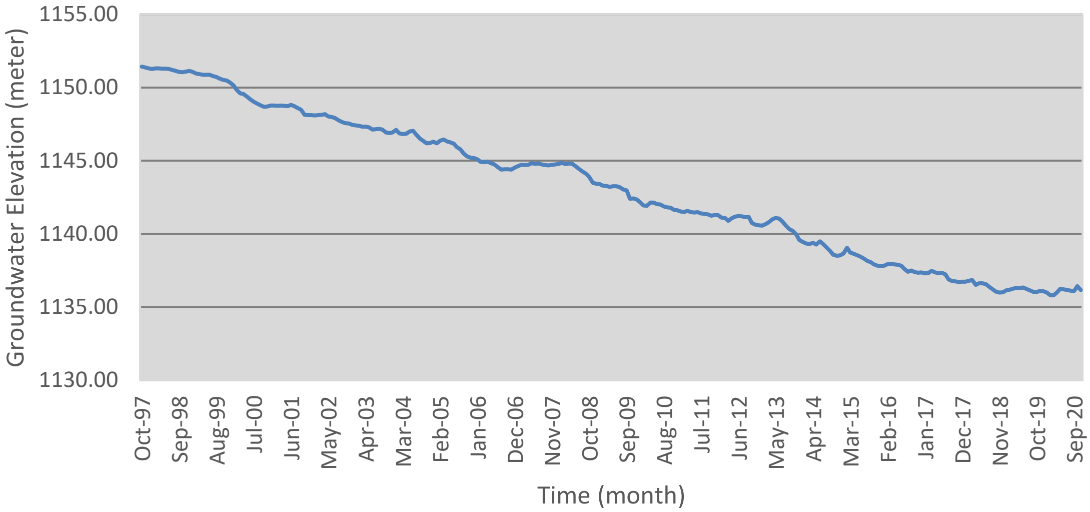

Fig. 7. Long-term monthly groundwater hydrograph in the Eshtehard alluvial aquifer; data is from 24 monitoring wells

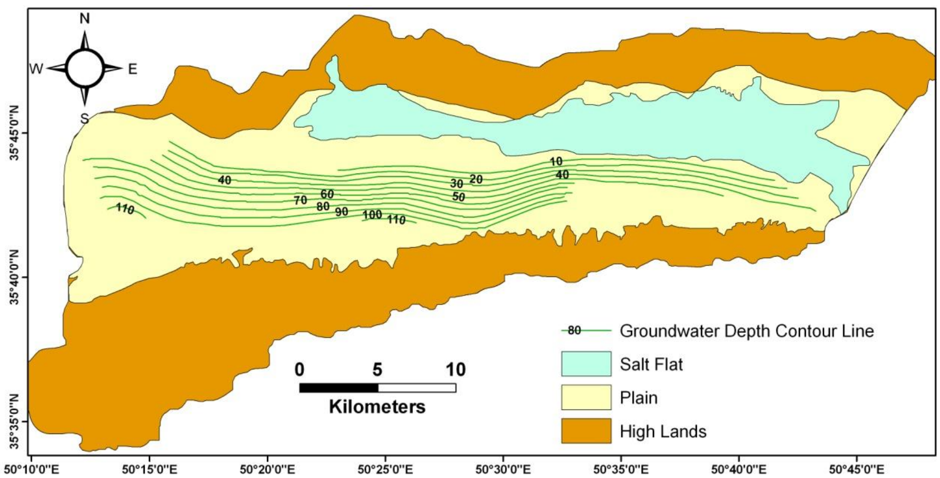

Fig. 8. Groundwater depth map of the study area (contours in meters)

According to the groundwater depth map, shallow water levels between 0.51 and 3.5 m below ground level are noticed in aquifer outlet, i.e., near the southern margins of the evaporating zone, and observed in 18.03% of monitoring network wells. Very deep-water levels more than 100 m below ground level are seen in some pockets spread in alluvial fan located in the southwestern aquifer near Ipak and Ghozlou villages and observed in 17.26% of monitoring network wells. Depth to water level ranging between 3.5-10 m below ground level and 50-100 m below ground level is observed in 9.8% and 25.07% of monitoring network wells, respectively. Most monitoring wells' depths (29.96%) range between 10 and 50 m below ground level. As is reflected in the map, the trend of depth to groundwater contours follows the east-west extension of the aquifer, and the depth to groundwater table increases from the north toward the southern parts of the aquifer.

https://doi.org/10.24191/scl.v20i2.11382

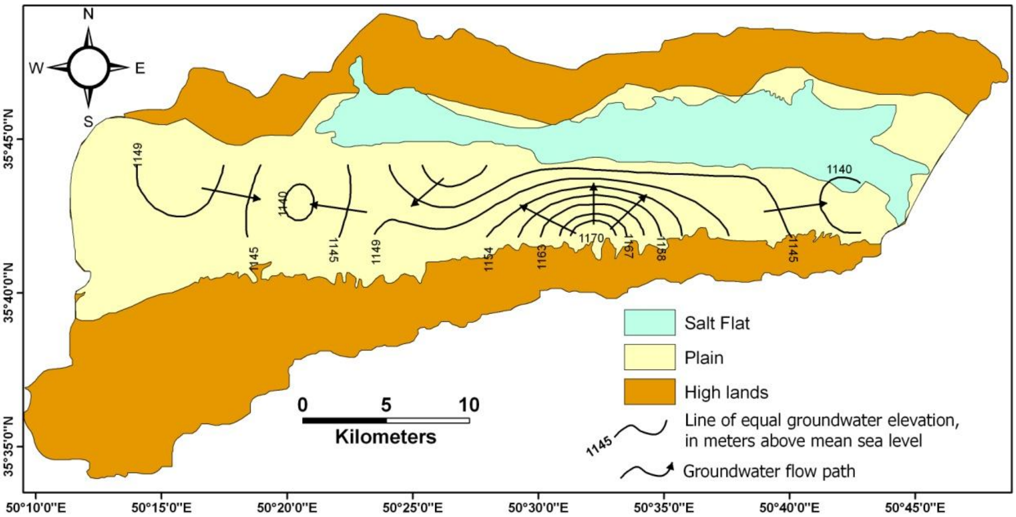

Fig. 9. Groundwater level contours (m a.m.s.l.)

According to the groundwater elevation map (Figure 9), water levels range between 1170 in southern parts and the recharge area to less than 1140 in northern areas and the outlet of the aquifer. The general groundwater flow direction is from south to north and west to east. Although, it is notable that due to the over-extraction of production wells around Eshtehard city and cultivation lands, the general groundwater flow direction has been tilted toward this extraction area, and in the west of Eshtehard city the groundwater flow direction has changed to an east-west direction. Meanwhile, a saline water intrusion from salt flats and the Shoor River has occurred due to declining water levels.

RESULT AND DISCUSSION

Groundwater recharge

Groundwater recharge rate estimation methods can be divided into main categories, i.e., physical and chemical methods (Sophocleous, 1991). Since groundwater recharge estimation is complex, especially in semiarid regions, confidence in recharge estimation improves when applying several methods (Delin et al., 2007; Walker et al., 2018). This study uses an integrated Water balance model (WB) and Water Table Fluctuation (WTF) methods to estimate the net Recharge into the Eshtehard aquifer. The water balance method focuses on the various components contributing to groundwater flow and storage changes (Figure 10). Marechal et al., 2006 changes in groundwater storage can be attributed to Recharge, irrigation return flow and groundwater inflow to the basin minus base flow (groundwater discharge to streams or springs), evapotranspiration from groundwater, pumping, and groundwater outflow from the basin. The equation presenting these components is adapted from Schicht and Walton (1961):

$$\boldsymbol{R} + \boldsymbol{RF} + \boldsymbol{Q}_{\boldsymbol{on}} = \boldsymbol{ET} + \boldsymbol{PG} + \boldsymbol{Q}_{\boldsymbol{off}} + \boldsymbol{Q}_{\boldsymbol{bf}} + \Delta \boldsymbol{S} \text{ (Equation 1)}$$

https://doi.org/10.24191/scl.v20i2.11382

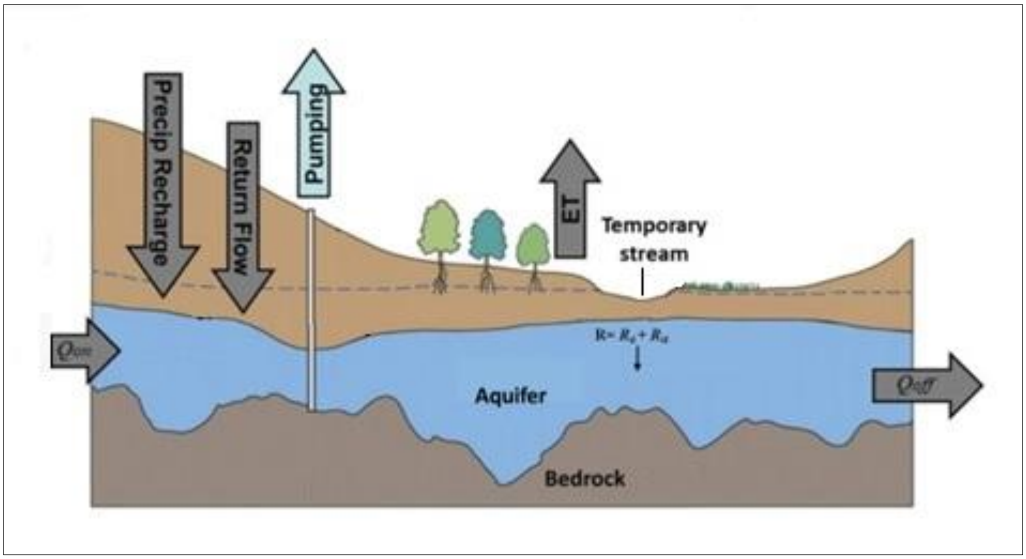

Fig. 10. Components of the groundwater budget in an unconfined aquifer

where R is total groundwater recharge (sum of direct recharge R_d through the unsaturated zone and indirect and localized Recharge R_{il}, respectively, from surface bodies and through local pathways like fractures), RF is sewage infiltration and irrigation return flow, Q_{on} and Q_{off} are groundwater flow onto and off the basin, ET is evaporation from the water table, PG is the abstraction of groundwater by pumping, Q_{bf} is baseflow (groundwater discharge to streams or springs). ΔS is a change in groundwater storage. Due to the significant thickness of the unsaturated zone overlying the unconfined aquifer in the study area – on average more than 50 m – the following simplifications can be made to the water budget:

- Groundwater discharge to surface water, Q_{bf}, via stream discharge or springs does not exist ($Q_{bf} = 0$). All groundwater discharge is via groundwater pumping.
- Evapotranspiration from the water table is negligible due to the immense depth of the groundwater table; therefore, this flow can be neglected, and Eq. 2 can be rewritten (Marechal et al. 2006):

$$\boldsymbol{R + RF + Q_{on} = PG + Q_{off} + \Delta S} \text{ (Equation 2)}$$

In the following sections, it is described the methods used for obtaining the different parameters in Eqs. (2), which are needed for the estimation of R.

Water table fluctuation (Δh)

Within this framework, the methodology used to determine the unknown groundwater storage is the WTF method (Amini & Homayounfar, 2017). This method has been selected based on the data availability and the study area's hydrogeological set-up. The WTF method is based on the premise that rises in groundwater levels in unconfined aquifers are due to recharge water arriving at the water table. It links the change in groundwater storage ΔS or net Recharge (R_{net}) with resulting water table fluctuations Δh:

$$\boldsymbol{\Delta s = R_{net} = S_y \,.\, \Delta h} \text{ (Equation 3)}$$

Where S_y is the specific yield (storage) of the unconfined aquifer.

https://doi.org/10.24191/scl.v20i2.11382

Techniques based on groundwater levels are among the most widely applied methods for estimating recharge rates (Scanlon et al., 2002). This is likely due to the abundance of available groundwater-level data and the simplicity of estimating recharge rates from temporal fluctuations or spatial patterns of groundwater levels. In the study area, the monitoring of the water table between 1997 and 2019 using 24 observation wells recorders shows that the aquifer displays well-identified large seasonal water-level fluctuations due to the percolation of water during the wet period through a relatively thick unsaturated zone (Fig 10). Since the detailed inventory of pumping wells and qanats was conducted between 2013 and 2014 (IWRMC, 2019), the study period was taken from October 2013 to September 2014 for the groundwater balance model. The Eshtehard Plain was portioned into 24 polygons (based on observation wells). For each polygon, Δh has been calculated based on monthly groundwater depth records of observation wells provided by TRWC (TRWC, 2019). The specific yield value (Sy) was obtained from two pumping tests by Tehran Regional Water Company (Abkhan, 2013). Because these values reflect an effective basin-wide process, they are insensitive to local heterogeneities in the aquifer system. According to Lv et al., 2021, Table 7 shows a wide range of values for specific yield (Sy) as a function of texture and aquifer materials. Based on this table and the observation well logs, the initial values of specific yield were determined for each polygon (Table 7). Then, by applying the Eq. 3, the net Recharge was calculated for that polygon. Finally, the total net Recharge for the Eshtehard plain was estimated at 14.38 million m^3/ year.

Table 7. The values of Sy as a function of texture and aquifer materials (Lv et al., 2021)

Material	Average specific yield	Minimum specific yield	Maximum specific yield
Clay	0.02	0.0	0.05
Silt	0.08	0.03	0.19
Sandy clay	0.07	0.03	0.12
Fine sand	0.21	0.10	0.28
Medium sand	0.26	0.15	0.32
Coarse sand	0.27	0.20	0.35
Gravelly sand	0.25	0.20	0.35
Fine gravel	0.25	0.21	0.35
Medium gravel	0.23	0.13	0.26
Coarse gravel	0.22	0.12	0.26

Lateral subsurface flows

For obtaining the groundwater flow (Q_{on} and Q_{off}), the Darcy equation was applied to compute net flow computation. Flow nets can be prepared by drawing a set of flow lines perpendicular to equipotential contour lines on groundwater-level contour maps. The flow lines will then form boundaries of stream tubes whereby it is assumed that groundwater flowing through an individual stream tube is neither losing nor gaining water from the neighbouring tube.

https://doi.org/10.24191/scl.v20i2.11382

Table 8. The values of Specific yield for the 24 observation wells in Eshtehard (After Abkhan, 2013 and Lv et al., 2021)

Observation Well No	Specific yield (S_y)	Observation Well No	Specific yield (S_y)	Observation Well No	Specific yield (S_y)
1	0.26	9	0.26	17	0.12
2	0.35	10	0.08	18	0.30
3	0.12	11	0.08	19	0.08
4	0.32	12	0.19	20	0.12
5	0.05	13	0.23	21	0.26
6	0.25	14	0.05	22	0.10
7	0.26	15	0.08	23	0.15
8	0.26	16	0.05	24	0.19

Darcy's law can compute the flow rate through a cross-sectional area of the aquifer by summing up flow rates through individual stream tubes. The groundwater flow rate through a stream tube at a selected cross-section can be computed by considering the discrete difference in hydraulic head for two successive contour lines, the stream tube's width and the aquifer's thickness. Darcy's law equation for the flow rate computation can be written as follows:

$$\boldsymbol{Q_s = K_s\ H\ W_s \frac{\Delta h}{L}} \text{(Equation 4)}$$

Q_s is the flow rate (horizontal) through the stream tube, K_s; horizontal hydraulic conductivity, H; Saturated aquifer thickness, W_s; width of the stream tube, Δh; discrete difference in groundwater level, and L; discrete distance between contour lines.

For each stream tube, the transmissivity is given by:

$$\mathbf{T = K_s . H} \text{(Equation 5)}$$

So, the flow rate equation for each stream tube can be rewritten:

$$\boldsymbol{Q_s = T\ W_s \frac{\Delta h}{L}} \text{(Equation 6)}$$

To apply the flow net computation method, transmissivity values and aerial distributions of groundwater levels are required. Transmissivity values for the Eshtehard Plain were determined from the transmissivity map of the study (Figure 5). Based on the groundwater elevation map for April 2014, the levels range from a high of about 1170 m above sea level in the south of Eshtehard plain to a low on the order of 1,140 m above sea level in the southwest of Eshtehard city. For each stream tube in the groundwater level contour lines, flow net computations have been carried out using Eq. 6. By summating the flows obtained for each tube, the total flow through the Eshtehard aquifer at the selected contour line was obtained. Transmissivity values representative of each set of selected contour lines has been considered. The results of this computation have been tabulated in Tables 9 and 10. Based on this computation, the average annual subsurface inflow and outflow are about 44.4 million m^3/ year and 18.76 million m^3/ year, respectively.

https://doi.org/10.24191/scl.v20i2.11382

Table 9. Values of transmissivity, hydraulic gradient, and subsurface inflow from to Eshtehard aquifer balance area in each stream tube

Section No.	Width (W) m	Hydraulic gradient ($\frac{\Delta H}{L}$)	Transmissivity (T) m^2/day	Average annual inflow (Million m^3)
I-1	425	0.00177	300	0.082
I-2	1830	0.002	600	0.802
I-3	1400	0.00103	1200	0.632
I-4	4350	0.00086	1125	1.536
I-5	2025	0.00521	1600	6.161
I-6	1850	0.0048	1900	6.158
I-7	2675	0.00453	1400	6.192
I-8	1500	0.00481	300	0.790
I-9	2195	0.0015	300	0.361
I-10	4825	0.00165	250	0.726
I-11	4540	0.00267	400	1.770
I-12	2100	0.0021	450	0.724
I-13	2475	0.0021	250	0.474
I-14	1525	0.00286	250	0.398
I-15	5820	0.00445	450	4.254
I-16	1400	0.00632	600	1.938
I-17	1600	0.00761	350	1.555
I-18	1100	0.00833	400	1.338
I-19	1290	0.00834	450	1.767
I-20	1630	0.00815	600	2.909
I-21	1900	0.0034	550	1.297
I-22	1775	0.00381	550	1.358
I-23	1525	0.00215	700	0.838
I-24	575	0.00254	700	0.373
		Total		44.433

https://doi.org/10.24191/scl.v20i2.11382

Table 10: Values of transmissivity, hydraulic gradient, and subsurface outflow from the Eshtehard aquifer balance area in each stream tube

Section No.	Width ($\boldsymbol{W}$) m	Hydraulic gradient ($\frac{\Delta H}{L}$)	Transmissivity ($\boldsymbol{T}$) m^2/day	Average annual outflow (Million m^3)
O-1	5230	0.00272	300	1.558
O-2	4345	0.00385	300	1.832
O-3	8050	0.00313	300	2.759
O-4	1690	0.00415	450	1.152
O-5	2225	0.00407	450	1.487
O-6	2380	0.00307	650	1.733
O-7	1460	0.00275	700	1.026
O-8	2145	0.00205	1900	3.049
O-9	3215	0.00203	1750	4.169
		Total		18.765

Groundwater pumping

Due to the absence of perennial surface water, the relatively low cost of drilling, and the possibility of getting water near the crops, groundwater is used for irrigation and industrial and domestic purposes in the Eshtehard area. Groundwater exploitations are performed via numerous production wells to cover regional needs. According to Abkhan Consulting Engineers (Abkhan, 2013) and Tehran Regional Water Company (TRWC, 2019), 119 deep and 359 shallow active pumping wells and 44 qanats operate in the alluvial aquifer. The total water withdrawal from all these artificial discharge points was measured during 2013 and 2014 and generalized for the whole year by the Abkhan for irrigation, domestic and industrial consumptions as 44.73, 3.78, and 6.73 million m^3/ year, respectively. Therefore, the total artificial groundwater withdrawal from the alluvial aquifer is about 56.91 million m^3/year. Recharge from the irrigation returns is estimated to be as high as 20% of the applied irrigation (44.73 million m^3/year from agricultural wells and 1.66 million m^3/year from qanats). Hence, Recharge from irrigation returns is 9.18 million m^3/year. Considerably percent of water for drinking and household uses turns to wastewater and, to some extent, percolates to the aquifer. The amount of return flow from production wells for municipal uses is estimated at 2.64 million m^3/year (70% of the total amount of groundwater abstracted for domestic uses). The total amount of groundwater abstracted for industrial uses is about 6.73 million m^3/year, estimated 70% of which 70% (4.66 million m^3/year) percolates to the aquifer.

Annual groundwater balance

Based on the different groundwater balance components obtained through the previous section (section 3.5), the annual groundwater budget of the Eshtehard aquifer was calculated based on Equation 3.2 from October 2013 to October 2014 and is presented in Table 11.

Table 11. Groundwater balance during one hydrological cycle

Water input (million m^3/year)		Water output (million m^3/year)	
Lateral groundwater fluxes	44.4	Subsurface outflows	18.76
Irrigation return	9.18	Agricultural abstractions	46.39
Domestic and industrial wells return	7.3	Domestic and industrial use	10.5
	60.88		75.65

https://doi.org/10.24191/scl.v20i2.11382

As illustrated in Table 11, a negative water budget of approximately 14.77 million m3/year is recorded in the aquifer system for 2014-2015. This can also be concluded from groundwater level fluctuations of the Eshtehard aquifer. Historical water level data shows a depletion of the aquifer at a rate of 0.7 meters per year in study areas, confirming that the overexploitation threshold has been reached in the Eshtehard aquifer.

CONCLUSION

According to geological and geoelectrical studies, the primary aquifer of Eshtehard is composed of alluvial deposits with a wide grain size range. Depth to the water table varies from less than one meter to about 120 meters. The general flow direction of groundwater is south to north and west to east. However, because of the over-extraction of production wells around Eshtehard city and agriculture areas, the overall groundwater flow direction has been slanted toward this extraction area, and the groundwater flow direction in the west of Eshtehard city has altered to the east-west. Meanwhile, a saline water intrusion from the salt flat and the Shoor River occurred due to a water level drop. Due to the study area's aridity, the Recharge estimation was challenging. An integrated water balance model (WB) and water table fluctuation (WTF) approaches were utilized in this work to estimate the net recharge into the Eshtehard aquifer. Using long-term hydrogeological data, various GIS maps were produced in the Arc GIS platform to calculate the groundwater budget components. Based on the groundwater balance, a negative water budget of approximately 14.77 million m3/year is recorded in the aquifer system for 2013-2014. Historical water level data shows a depletion of the aquifer at a rate of about 0.7 meters per year in study areas, confirming that the overexploitation threshold has been reached in the Eshtehard aquifer. In computing groundwater's water balance, using the Water Table Fluctuation method, a relation has been made between the values of specific yield and groundwater table fluctuations. However, in the groundwater balance study, an effort has been made to establish a logical relationship between the data availability and the method complexity to demonstrate the reality of the system in the best possible way. This result allows decision-makers to assign the extractable discharge quantity to guarantee the aquifer's long-term management. In this context, even though there are enough piezometer wells (a total of 24 with high density; almost 2 in every 25 km^2), there is not enough data on observation wells and pumping tests to evaluate aquifer characteristics. It will lead to sufficient clearance of the Eshtehard aquifer-specific yield and transmissivity, which is necessary to improve the findings of this research.

ACKNOWLEDGEMENT

The authors would like to thank the Universiti Putra Malaysia and Tehran Regional Water Company. The authors are also grateful to the editors and the reviewers for making time to review the manuscript.

FUNDING DECLARATION

This research did not receive any specific grant from the public, commercial, or not-for-profit funding agencies.

AUTHORS CONTRIBUTIONS

Leila Khodapanah: Writing original draft preparation Methodology data collection, interpretation of results, Study conception and design, Negar Anvarizadeh: Study conception and design, Kourosh Mohammadi: Data interpretation. Sikiru Surajudeen: conceptualization, interpretation of results, Data Accuracy, Hassan Soleimani: Supervision and conceptualization. All authors reviewed the results and approved the final version of the manuscript.

https://doi.org/10.24191/scl.v20i2.11382

REFERENCES

[1] P. Sudegi and H. Khairy, "Multi-Method Estimation of Groundwater Recharge in Semi-Arid Regions: A Comparative Analysis of Physical, Chemical, and Isotopic Approaches," *Groundwater for Sustainable Development,* p. 101605, 2026.

[2] S. A. Vaghefi *et al.*, "The future of extreme climate in Iran," *Scientific reports,* vol. 9, no. 1, p. 1464, 2019.

[3] L. Khodapanah and W. N. A. Sulaiman, "Groundwater Quality Mapping of an Alluvial Aquifer, Eshtehard, Iran," *VOL. 19 (S) OCT. 2011,* p. 59, 2011.

[4] E. Fijani and S. Meysami, "Assessment of hydrochemical characteristics and groundwater suitability for drinking and irrigation purposes in Garmsar Plain, Iran," *Geopersia,* vol. 13, no. 1, pp. 83-102, 2023.

[5] D. Tien Bui *et al.*, "Shallow landslide prediction using a novel hybrid functional machine learning algorithm," *Remote Sensing,* vol. 11, no. 8, p. 931, 2019.

[6] S. A. Ganiyu, J. O. Olutoki, M. Q. Alkahtani, and N. A. Khan, "Comparative assessment of groundwater quality and stability around active and closed dumpsites in Ibadan, Nigeria," *Scientific Reports,* 2026.

[7] K. Madani, "Water management in Iran: what is causing the looming crisis?," *Journal of environmental studies and sciences,* vol. 4, no. 4, pp. 315-328, 2014.

[8] M. F. Bierkens and Y. Wada, "Non-renewable groundwater use and groundwater depletion: a review," *Environmental Research Letters,* vol. 14, no. 6, p. 063002, 2019.

[9] X. Jia, D. Hou, L. Wang, D. O'Connor, and J. Luo, "The development of groundwater research in the past 40 years: A burgeoning trend in groundwater depletion and sustainable management," *Journal of Hydrology,* vol. 587, p. 125006, 2020.

[10] J. Du *et al.*, "Groundwater depletion and degradation in the North China Plain: Challenges and mitigation options," *Water,* vol. 16, no. 2, p. 354, 2024.

[11] M. M. Ghaleni and K. Ebrahimi, "Effects of human activities and climate variability on water resources in the Saveh plain, Iran," *Environmental monitoring and assessment,* vol. 187, no. 2, pp. 1-17, 2015.

[12] A. Singh, S. N. Panda, V. N. Uzokwe, and P. Krause, "An assessment of groundwater recharge estimation techniques for sustainable resource management," *Groundwater for Sustainable Development,* vol. 9, p. 100218, 2019.

[13] S. B. Mafilika, "Using stable isotopes to understand relative contributions of evaporation and evapotranspiration on groundwater recharge in the Verlorenvlei catchment, west coast, South Africa," Stellenbosch: Stellenbosch University, 2021.

[14] S. Ganiyu, V. Uwem, J. Olutoki, O. Onakoya, K. Are, and B. Badmus, "Investigation of groundwater quality and stability nearby active municipal solid waste dumpsite in Ibadan Metropolis, Nigeria," *International Journal of Energy and Water Resources,* vol. 9, no. 4, pp. 2491-2515, 2025.

[15] Z. Zhang, W. Wang, C. Gong, and M. Zhang, "A comparison of methods to estimate groundwater recharge from bare soil based on data observed by a large-scale lysimeter," *Hydrological Processes,* vol. 34, no. 13, pp. 2987-2999, 2020.

[16] R. C. Doble and R. S. Crosbie, "Current and emerging methods for catchment-scale modelling of recharge and evapotranspiration from shallow groundwater," *Hydrogeology journal,* vol. 25, no. 1, p. 3, 2017.

[17] D. Walker *et al.*, "Insights from a multi-method recharge estimation comparison study," *Groundwater,* vol. 57, no. 2, pp. 245-258, 2019.

[18] Y. Xu and H. E. Beekman, "Groundwater recharge estimation in arid and semi-arid southern Africa," *Hydrogeology Journal,* vol. 27, no. 3, pp. 929-943, 2019.

[19] V. H. R. Coelho *et al.*, "Alluvial groundwater recharge estimation in semi-arid environment using remotely sensed data," *Journal of Hydrology,* vol. 548, pp. 1-15, 2017.

https://doi.org/10.24191/scl.v20i2.11382

[20] F. Manna, S. Murray, D. Abbey, P. Martin, J. Cherry, and B. Parker, "Spatial and temporal variability of groundwater recharge in a sandstone aquifer in a semi-arid region," *Hydrology and Earth System Sciences Discussions,* vol. 2018, pp. 1-36, 2018.
[21] M. K. Matta *et al.*, "Determination of non-transferrin bound iron, transferrin bound iron, drug bound iron and total iron in serum in a rats after IV administration of sodium ferric gluconate complex by simple ultrafiltration inductively coupled plasma mass spectrometric detection," *Nanomaterials,* vol. 8, no. 2, p. 101, 2018.
[22] J. Porhemmat, M. Nakhaei, M. A. Dadgar, and A. Biswas, "Investigating the effects of irrigation methods on potential groundwater recharge: A case study of semiarid regions in Iran," *Journal of Hydrology,* vol. 565, pp. 455-466, 2018.
[23] S. Andaryani, V. Nourani, B. Pradhan, T. Jalali Ansarudi, F. Ershadfath, and A. Torabi Haghighi, "Spatiotemporal evaluation of future groundwater recharge in arid and semi-arid regions under climate change scenarios," *Hydrological Sciences Journal,* vol. 67, no. 6, pp. 979-995, 2022.
[24] M. Karamouz, J. Teymoori, and M. Olyaei, "A Spatial non-stationary based site selection of artificial groundwater recharge: a case study for semi-arid regions," *Water Resources Management,* vol. 35, no. 3, pp. 963-978, 2021.
[25] M. G. Zamani, A. Moridi, and J. Yazdi, "Groundwater management in arid and semi-arid regions," *Arabian Journal of Geosciences,* vol. 15, no. 4, p. 362, 2022.
[26] T. S. G. Ferreira and J. A. Cirilo, "Remote sensing data for estimating groundwater recharge: A systematic review," *Sustainability,* vol. 18, no. 4, p. 1830, 2026.
[27] R. Noori *et al.*, "Decline in Iran's groundwater recharge," *Nature communications,* vol. 14, no. 1, p. 6674, 2023.
[28] H. R. Nassery, N. Zeydalinejad, F. Alijani, and A. Shakiba, "A proposed modelling towards the potential impacts of climate change on a semi-arid, small-scaled aquifer: a case study of Iran," *Environmental Monitoring and Assessment,* vol. 193, pp. 1-32, 2021.
[29] H. Ketabchi, D. Mahmoodzadeh, E. Valipour, and T. Saadi, "Uncertainty-based analysis of water balance components: a semi-arid groundwater-dependent and data-scarce area, Iran," *Environment, Development and Sustainability,* vol. 26, no. 12, pp. 31511-31537, 2024.
[30] S. M. Hosseini, E. Parizi, B. Ataie-Ashtiani, and C. T. Simmons, "Assessment of sustainable groundwater resources management using integrated environmental index: Case studies across Iran," *Science of the total environment,* vol. 676, pp. 792-810, 2019.
[31] L. Geneviève, C. Romain, and B. Marie-Amélie, "Water-table fluctuation method for assessing aquifer recharge: application to Canadian aquifers and comparison with other methods," *Hydrogeology Journal,* vol. 28, no. 2, pp. 521-533, 2020.
[32] M. B. Addisie, "Groundwater recharge estimation using water table fluctuation and empirical methods," *H2Open Journal,* vol. 5, no. 3, pp. 457-468, 2022.
[33] S. H. Sadeghi and Z. Hazbavi, "Land degradation in Iran," in *Global Degradation of Soil and Water Resources: Regional Assessment and Strategies*: Springer, 2022, pp. 287-314.
[34] F. Pasand, H. M. Nasb, and M. A. Ehyaei, "Application of Thermal Comfort Indicators in Climate Design (Case Study: Yazd Township)," *International Journal of Applied Arts Studies (IJAPAS),* vol. 8, no. 2, pp. 29-48, 2023.
[35] M. A. Al-Dabbas, A. A. Al-Zubaidi, and R. Al-Khafaji, "Impact of climate changes on the hydrochemistry of Razaza Lake and Rahaliya–Shithatha Springs–Central Iraq," *J Environ Earth Sci,* vol. 5, no. 6, pp. 106-115, 2015.
[36] M. Yousefi and V. Nykänen, "Data-driven logistic-based weighting of geochemical and geological evidence layers in mineral prospectivity mapping," *Journal of Geochemical Exploration,* vol. 164, pp. 94-106, 2016.
[37] L. Tomassetti, A. Benedetti, and M. J. S. G. Brandano, "Middle Eocene seagrass facies from Apennine carbonate platforms (Italy)," vol. 335, pp. 136-149, 2016.
[38] A. Aghanabati, *Geology of Iran*. Geological survey of Iran, 2004.

https://doi.org/10.24191/sl.v20i2.11382

[39] T. R. W. Authority, "Semicomprehensive groundwater studies of Eshtehard plain, Vol. 1, 2 and 3, Abkhan Consulting Eng," ed: Co, 2005.
[40] J. P. Clement IV *et al.*, "Association and stoichiometry of KATP channel subunits," *Neuron,* vol. 18, no. 5, pp. 827-838, 1997.
[41] A. T. Tizro, K. S. Voudouris, M. Salehzade, and H. Mashayekhi, "Hydrogeological framework and estimation of aquifer hydraulic parameters using geoelectrical data: a case study from West Iran," *Hydrogeology Journal,* vol. 18, no. 4, pp. 917-929, 2010.
[42] A. A. Moghaddam and M. A. Najib, "Hydrogeologic characteristics of the alluvial tuff aquifer of northern Sahand Mountain slopes, Tabriz, Iran," *Hydrogeology Journal,* vol. 14, no. 7, pp. 1319-1329, 2006.
[43] S. H. Ahmadi and A. Sedghamiz, "Application and evaluation of kriging and cokriging methods on groundwater depth mapping," *Environmental monitoring and assessment,* vol. 138, no. 1, pp. 357-368, 2008.